CNWRA *A center of excellence in earth sciences and engineering*

A Division of Southwest Research Institute™
6220 Culebra Road • San Antonio, Texas, U.S.A. 78228-5166
(210) 522-5160 • Fax (210) 522-5155

February 15, 2001
Contract No. NRC–02–97–009
Account No. 20.01402.671

U.S. Nuclear Regulatory Commission
ATTN: Mrs. Deborah A. DeMarco
Two White Flint North
11545 Rockville Pike
Mail Stop T8 A23
Washington, DC 20555

Subject: Programmatic Review of Papers

Dear Mrs. DeMarco:

The enclosed papers, which will be submitted for presentation at the 38th U.S. Rock Mechanics Symposium to be held in Washington, DC on July 7–10th, 2001 are being submitted for programmatic review. The titles of these papers are:

> *"Simulation of Earthquake Effects on Underground Excavations Using Discontinuous Deformation Analysis (DDA)"* by S. Hsiung and G.H. Shi
>
> and
>
> *"Discontinuous Deformation Analysis (DDA) with nth Order Polynomial Displacement Functions"* by S. Hsiung

Discontinuous Deformation Analysis (DDA) computer code is being used to investigate the effects of earthquake ground motions on rockfall in emplacement drifts during pre-and post-closure periods of the proposed repository at Yucca Mountain under heated conditions. The goal of the study is to relate the magnitude of ground motion with the extent of rockfall. The result of the study will be used as input for the SEISMO module in the NRC Total-System Performance Assessment Code.

The first paper documents aspects of the rockfall potential when an emplacement drift is subjected to earthquake ground motion. The version of the DDA code used to conduct the earthquake effect study was developed based on a linear (first order) polynomial displacement function. In a newer version of the DDA code, the first-order polynomial function has been made a special case. Any order of polynomial displacement function can now be selected to approximate displacement in a rock block. The verification of this new DDA code is presented in the second paper.

Washington Office • Twinbrook Metro Plaza #210
12300 Twinbrook Parkway • Rockville, Maryland 20852-1606

These papers present results of work conducted by the CNWRA as parts of the Repository Design and Thermal-Mechanical Effects Key Technical Issue. These papers are products of the CNWRA and do not necessarily reflect the views or regulatory position of the NRC.

Please advise me of the results of your programmatic review. Your cooperation in this matter is appreciated.

Sincerely,

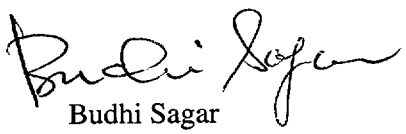

Budhi Sagar
Technical Director

Attachment
cc: J. Linehan
W. Reamer
B. Meehan
E. Witt
J. Greeves
T. Essig
S. Wastler
D. Brooks
K. Stablein
M. Nataraja
B. Jagannath
W. Patrick
CNWRA Dirs
CNWRA EMs
G.I. Ofoegbu
S. Hsiung

Simulation of Earthquake Effects on Underground Excavations Using Discontinuous Deformation Analysis (DDA)

S.M. Hsiung
Center for Nuclear Waste Regulatory Analyses, Southwest Research Institute

Gen-Hua Shi
Consultant, Belmont, California

ABSTRACT: In seismic prone regions, consideration of earthquake effects is an important aspect in designing underground civil structures, storage, and power stations. Also, potential earthquake effects on stability of underground openings that will be used for disposal of high-level waste in a geologic repository may have performance implications. The Discontinuous Deformation Analysis (DDA) computer code is extended to model earthquake effects on underground excavations in jointed rock media. In addition, the effects of uncertainties in rock joint characterization are incorporated in the analysis. The analysis results indicate that DDA is appropriate for analyzing stability of underground excavations subjected to earthquakes taking into account the uncertainties in rock joint data.

1 INTRODUCTION

In seismic prone regions, consideration of earthquake effects is an important aspect for design of underground civil structures, storage, and power stations. Also, potential effects of earthquakes on stability of underground openings that will be used for disposal of high-level waste in a geologic repository may have implications for performance.

Compared with surface constructions, there has been relatively little research effort expended and, consequently, relatively less understanding on the seismic performance of underground excavations. One reason for little research effort stems from the notion that underground excavations are less susceptible to dynamic loadings than surface facilities (Sharma and Judd, 1991). Another reason, perhaps the most important one, is that very few data are available on damage of subsurface structures due to earthquakes.

During the past two decades, numerical techniques have been developed sufficiently to permit meaningful assessment of dynamic effects on underground excavations. In this regard, both continuum and discontinuum approaches are used in analyzing rock-mass responses to earthquake ground motions. Continuum approach provides some understanding of stresses and displacements of excavations subjected to earthquake ground motion for rock media with relatively fewer discontinuities or for excessively fractured rock media; whereas discontinuum approach is more appropriate for studying excavations in moderately jointed rock media where systems of rock blocks are formed.

The presence of joints not only reduces modulus and strength of rock media but also provides planes of weakness on which slip, separation and rigid body translation of blocks can occur preferentially (Kana et al., 1989). Excessive slippage along joints may have serious consequences on stability of excavations. Observations indicate that damage to underground excavations due to oscillatory motions or shaking in jointed rock media is manifested as displacements along joint surfaces, perhaps involving rockfalls, cracking, and spalling of the rock media (Kana et al., 1989). Depending on the state of stresses on joints, and strengths and material properties of intact rock and joints, progressive accumulation of damage resulting from slippage along joints weakens a rock mass leading to instability of the excavations (Brown and Hudson, 1974, Barton and Hansteen, 1979, Hsiung et al., 1992, Hsiung et al., 1999). Furthermore, stability of excavations can be influenced further through accumulation of permanent deformations around the excavations when subjected to repeated episodes of earthquakes. Therefore, if underground facilities are to be located in seismically active regions and are expected to experience several episodes of seismic activity during their intended service life span, consideration of the effects of repeated seismic loads in the design of such facilities seems to be necessary.

Two discontinuum methods are currently available for analyzing responses of rock media surrounding underground excavations: distinct element method (DEM) and discontinuous deformation analysis (DDA). This paper focuses on the effects of earthquakes on underground excavations in a jointed rock medium using the DDA.

Another important aspect of analyzing the stability of underground excavation using either DEM or DDA is the potential effect of uncertainties in parameters required to specify the joint patterns. Several methods are available for incorporating parameter uncertainties into structural analyses and design (e.g. Wu et al., 1990); the Monte Carlo method used in this paper is the most general.

2 DISCONTINUOUS DEFORMATION ANALYSIS

DDA (Shi, 1996) is the block system version of the finite element method (FEM). It involves a finite element type of mesh where each element represents a real isolated block, bounded by pre-existing joints (discontinuities). Although DDA seems to resemble the distinct element method in that it accounts for joint contact behavior, mathematically it parallels FEM in the following aspects (Shi, 1996)

- DDA establishes its equilibrium equations by minimizing the total potential energy of the system;
- DDA uses displacements as unknown for the simultaneous equations; and
- Stiffness, mass, and loading matrices of individual blocks are calculated independently and added to the global matrix of the entire system.

The blocks simulated in DDA can be of any shape (both convex and concave). An implicit solution algorithm is adopted in the DDA. The large displacements of the blocks are accounted for by the use of a time step scheme; at the end of each time step, the equilibrium is reached by minimizing the total potential energy, and block geometry is updated. The deformed block geometry and the resulting state of stresses from this time step is used as the initial condition for the next time step.

In each time step, assuming the stresses and strains within a block are constant, the x- and y-direction displacements (u,v) at any point (x,y) of a block can be represented using the first-order polynomial approximation by six displacement variables (Shi, 1996)

$$\begin{bmatrix} u \\ v \end{bmatrix} = \begin{bmatrix} 1 & 0 & y_0 - y & x - x_0 & 0 & \frac{y - y_0}{2} \\ 0 & 1 & x - x_0 & 0 & y - y_0 & \frac{x - x_0}{2} \end{bmatrix} \begin{bmatrix} u_0 & v_0 & r_0 & \varepsilon_x & \varepsilon_y & \gamma_{xy} \end{bmatrix}^T \tag{1}$$

where (x_0, y_0) is the reference point in the block (for convenience, centroid of the block is normally used); (u_0, v_0) is the rigid body translation of point (x_0, y_0); r_0 is the rotation angle of the block with respect to point (x_0, y_0); and ε_x, ε_y, and γ_{xy} are the normal and shear strains of the block. Eq. (1) can be generalized as

$$\begin{bmatrix} u_i \\ v_i \end{bmatrix} = [W_i][D_i] = \begin{bmatrix} t_{11}^i & t_{12}^i & t_{13}^i & t_{14}^i & t_{15}^i & t_{16}^i \\ t_{21}^i & t_{22}^i & t_{23}^i & t_{24}^i & t_{25}^i & t_{26}^i \end{bmatrix} \begin{bmatrix} d_{1i} \\ d_{2i} \\ d_{3i} \\ d_{4i} \\ d_{5i} \\ d_{6i} \end{bmatrix} \tag{2}$$

where the subscript i denotes the ith block, $[W_i]$ is the transformation function, and $[D_i]$ contains the variables mentioned earlier.

Determination of block deformation involves solving for variables $[D_i]$. The simultaneous equations for the system is

$$[K]_G[D]_G = [F]_G \tag{3}$$

where $[K]_G$ is the system stiffness matrix and $[F]_G$ is the force or load matrix. Contribution to $[K]_G$ and $[F_G]$ is from strains, initial stresses, body forces, inertia force, loading conditions, and displacement constraints of individual blocks; and contacts between blocks.

To model a blocky system, a complete solution has to satisfy both equilibrium and compatibility conditions. The DDA uses an open-close iteration criterion to fulfill the compatibility conditions between blocks by solving a set of algebraic inequalities through iterations within a given time step (Shi, 1996). The open-close iteration process continues until no tension or penetration occurs at all conditions of contact modes before the calculation proceeds to the next time step. Based on natural contact phenomena, three basic contact modes can be identified: open, sliding, and locking.

In DDA, Coulomb's Law is applied to assess the contact conditions. At every iteration, each contact is evaluated to determine if

- Normal force at the contact is greater than or equal to the contact tensile strength;
- Shear contact force is smaller than the contact shear strength multiplied by the half length of the block edge where this contact is located, when the normal contact force is compressive; or
- Shear contact force is equal to or greater than the contact shear strength multiplied by the half length of the block edge where this contact is located, when the normal contact force is compressive.

If the first condition is satisfied, the contact is judged as open and no normal spring is applied. When the second condition is met, the contact is essentially locked such that no sliding between point P_1 and line $\overline{P_2P_3}$ has occurred. Under this condition, both normal and shear stiffnesses are simulated using normal and shear springs at the contact. If the third condition is met, P_1 slides along $\overline{P_1P_2}$; a normal spring is added and a pair of friction forces at the contact are added to the system force matrix $[F]_G$. The contribution of the added contact springs should be included in the system stiffness matrix $[K]_G$ and force matrix $[F]_G$ to account for the kinematics between blocks in the system.

3 DATA INPUT AND MODEL GEOMETRY

Simulation of earthquake ground motions using DDA was introduced by Shi (1999) to study stability of blocky rock slopes. The same concept is adopted here to investigate rockfall and stability of underground excavations. This investigation was conducted using a joint pattern that contains three sets of joints. The joint information considered in the analysis included joint dip direction, joint dip angle, joint spacing, joint length, and bridge (gap) length and is listed in Table 1. To use this statistical information on joint parameters, a Monte Carlo technique was adopted to generate sample joint patterns. Note that each sample generated is an equally likely realization of joints that honor the information in Table 1. In generating these realizations, the joint spacing, length, and gap were assumed to be uniformly distributed; other appropriate distributions such as normal and lognormal can also be incorporated. Uncertainties in joint dip angle and dip direction were not incorporated in this study to avoid producing overly complicated DDA block models. Figure 1 shows a realization of joint distribution generated stochastically for constructing DDA block model. The joint lines in the figure are bounded by the inner edges of the boundary frame on all sides.

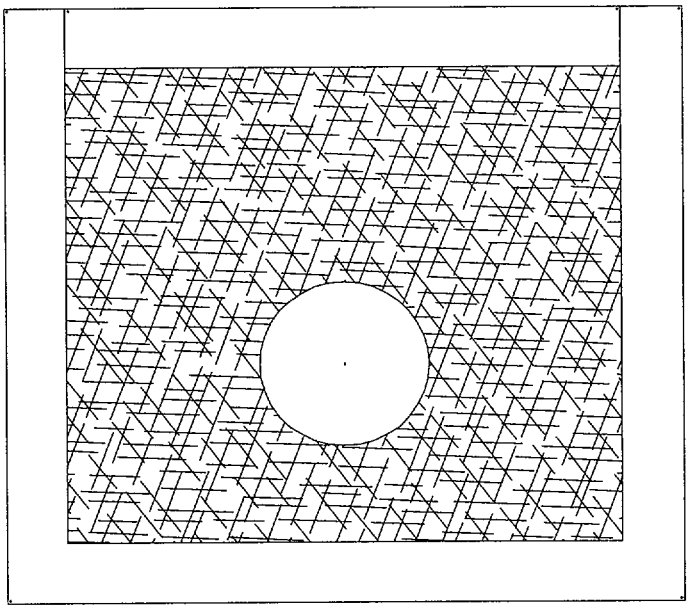

Figure 1 Joint distribution using data from Table 1

The joint distribution realizations similar to that in Figure 1 were further processed to form blocks (Fig. 2) for discontinuous deformation modeling. A tree cutting procedure was used to remove joints or portions of joints that did not contribute to the formation of blocks since DDA deals with blocks only. Figure 2 shows three DDA block realizations developed after non-intersecting joints were removed. All three realizations used the same joint information listed in Table 1 and have equal likelihood of being actually present. In a full application of the Monte Carlo technique, a

Table 1 Information of joint sets used in the analysis

Joint Set	Dip Angle, degrees	Dip Direction, degrees	Mean Spacing, m	Standard Deviation of Spacing, m	Mean Length, m	Standard Deviation of Length, m	Mean gap, m	Standard Deviation of Gap, m
1	79	270	0.3	0.105	1.8	0.63	0.4	0.14
2	81	230	0.3	0.105	2.4	0.84	0.3	0.105
3	5	45	0.5	0.175	1.8	0.63	0.5	0.175

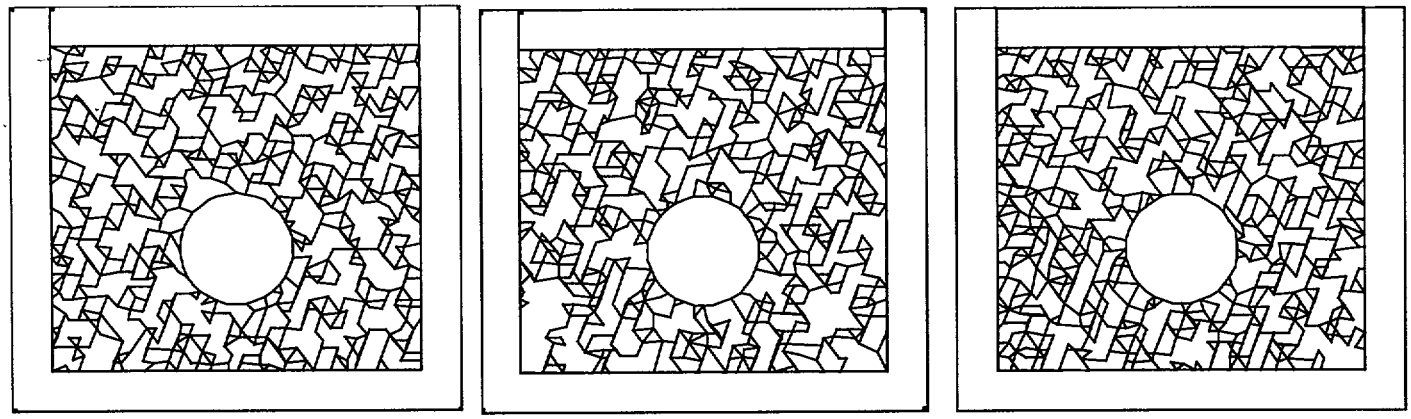

(a) DDA Block Realization 1 (b) DDA Block Realization 2 (c) DDA Block Realization 3

Figure 2 Three DDA block realizations developed using the data from Table 1 considering perturbations

sufficient number (anywhere from 50-100) of realizations should be analyzed. For determining the sufficient number of realizations, one should plot selected statistics (e.g., mean damage) versus number of realizations. When these statistics stop varying as the number of realizations, one has enough samples. In this paper, only three realizations are analyzed to show the potential effect of joint parameter uncertainties. The computational burden increases by a factor equal to the number of realizations when the Monte Carlo technique is used. However, the explicit incorporation of parameter uncertainties into the DDA can lead to a risk-based design and can provide quantitative estimate of confidence in analysis results.

The circular space in the figure represents an excavation of 5.5 m in diameter. The azimuth of the orientation of the excavation simulated is 75 degrees. The frame placed outside the block system was intended to provide horizontal and vertical displacement constraints; displacement was not allowed in the direction normal to either side of the frame. Rock blocks in contact with the inner edges of the boundary frame were allowed to slide along the contacted edge.

The unit weight, Young's modulus, and Poisson's ratio for rock blocks in the realizations of Figure 2 are assumed to be 2.27 tons/m^3 (2,270 kg/m^3), 3×10^5 tons/m^2 (3.0 Gpa), and 0.21, respectively. A friction angle of 39 degrees and zero cohesion were assigned to the joints in all joint sets. A total of 20,000 to 22,000 time steps were used for each analysis and the duration of each time step was 0.002s.

In DDA, simulation of earthquake motion was implemented by applying ground accelerations directly to the blocks/elements. The ground acceleration signal used in the study was a three-

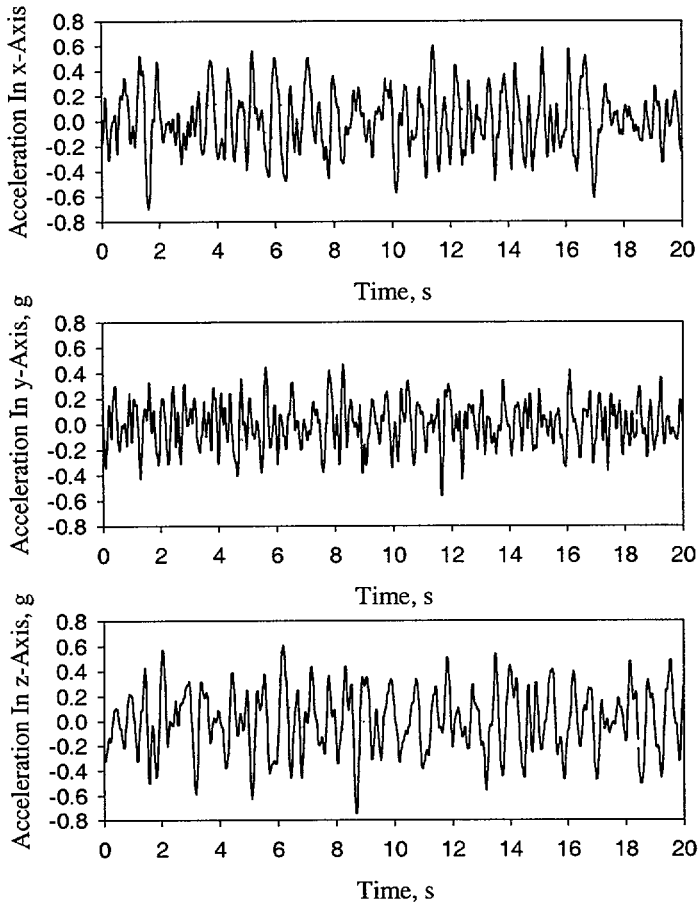

Figure 3 Earthquake acceleration time history

dimensional (3D) acceleration time history developed by the California Department of Transportation for the Yerba Buena Island Tunnel seismic retrofit program (Shi, 1999, Law and Lam, 1999). Total duration of this time history record is 50s out of which the record from 10 to 30s was used in this study. The accelerations in this duration encompass the major portion of the ground motion. Figure 3 shows the extracted data along x-, y-, and z-directions.

This paper examines the feasibility of using DDA as a tool for assessing the vulnerability of underground excavations to ground motions and presents results of the effects of earthquake magnitudes on stability of excavation. Different magnitudes of earthquake were obtained by scaling the ground acceleration time history shown in Figure 3 to different levels. Also examined in this paper are effects of repeated episodes of earthquakes.

4 RESULTS AND DISCUSSION

Response of the rocks surrounding excavations to ground motions is very complicated. Studies indicate that a rock mass may be damaged by ground motions (Brown and Hudson, 1974, Sharma and Judd, 1991, Hsiung et al., 1992, 1999). This damage can be characterized in the form of cracking, spalling, excessive joint shear displacement, and rockfall. The form of damage may be related to the characteristics of rock media, state of stresses, and, perhaps, the type and extent of supports used.

In the moderately jointed rock media where systems of rock blocks are formed, damage such as spalling, excessive joint shear displacement, and rockfall may be of concern under earthquakes if excavations are not sufficiently supported. The damage may be further influenced by geometries of blocks surrounding excavations. As indicated earlier, Figure 2 shows three DDA block realizations developed through Monte Carlo sampling using the joint information presented in Table 1. The behavior of the unsupported excavations for these realizations of joint patterns subjected to the same seismic ground motions is shown in Figure 4. The acceleration time history in Figure 3 with a 1/5 scaling on amplitudes was used in these realizations. Among the three, excavation in realization 2 experienced the most extensive rockfall from roof while excavation in realization 3 suffered the least damage (Fig. 4). Although the extent of rockfall for the excavation in realization 1 appears the same as that in realization 3, excessive shear displacements along joints were observed in rocks at the top left side of the excavation; indicating that the excavation in realization 1 is less stable.

These results indicate clearly that the variations associated with the joint parameters play a very important role in the stability of underground excavations when they are subjected to seismic ground motions. Furthermore, these results identify potential effects of inherent variability in rock media on excavation stability. If these variations are not accounted for in an analysis, critical responses may not be captured properly. As a result, the stability of excavations may be over- or under-estimated leading to an insufficient or uneconomical design of ground support. In order to assess earthquake damage and subsequently determine adequate support requirements, the responses of a sufficient number of realizations should be examined to quantify the range of possible damage. Proper support requirements can then be derived to contain damage. Damage indicators selected should be consistent with the nature of the problem analyzed.

Although variations in joint directions and joint dips are not considered specifically in this study their importance can also be inferred since they could potentially affect the size and shape of rock blocks. It should be noted that most rock blocks in 3D may be constrained by the neighboring blocks in all three dimensions while the rock blocks analyzed in 2D are constrained only in two dimensions. Consequently, results from 2D analysis are normally more conservative than those from 3D analysis. In other words, the predicted extent of rockfall using 3D analysis may be less than that observed in Figure 4.

Figure 5 shows rockfall for realization 1. Acceleration time history input used for Figure 5 is

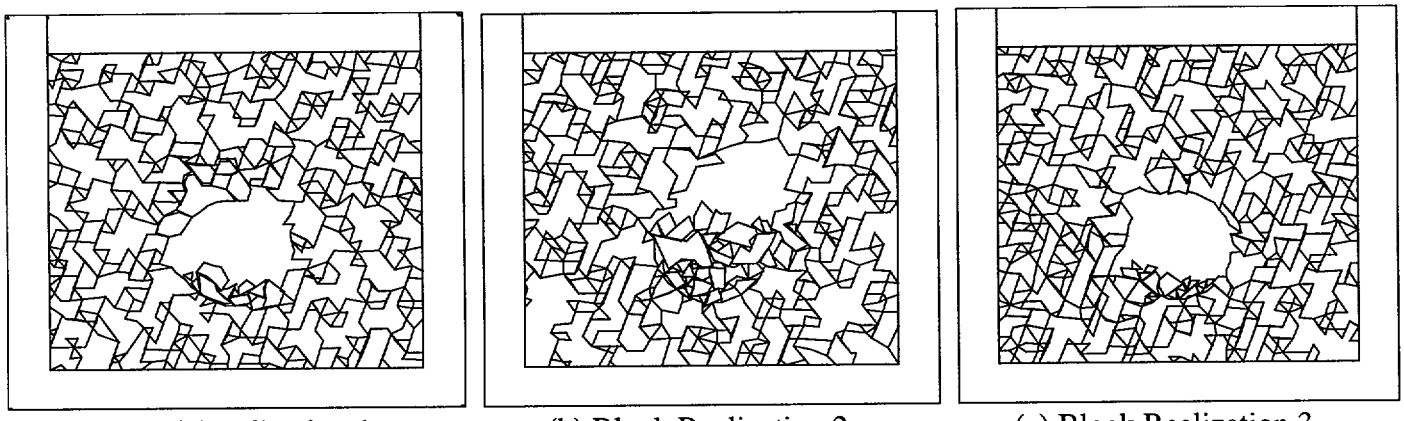

(a) Block Realization 1 (b) Block Realization 2 (c) Block Realization 3

Figure 4 Effects of block geometry on stability of underground excavations

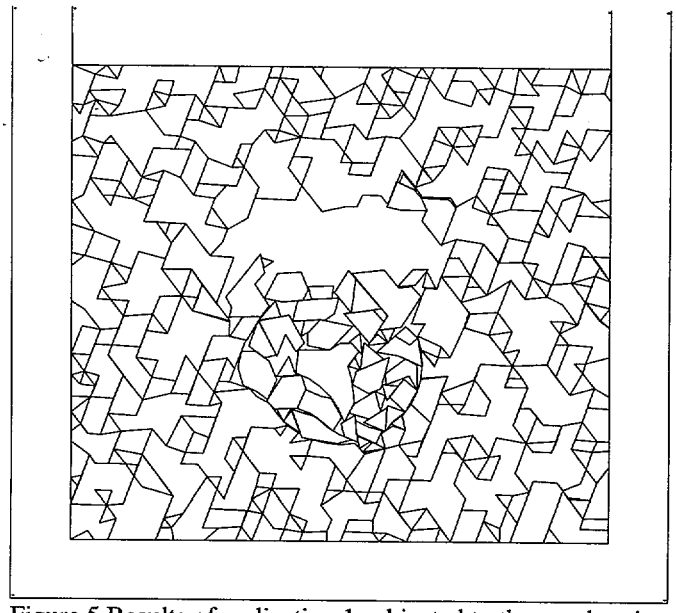

Figure 5 Results of realization 1 subjected to the acceleration time history shown in Figure 3 with no scaling applied to the amplitude and duration

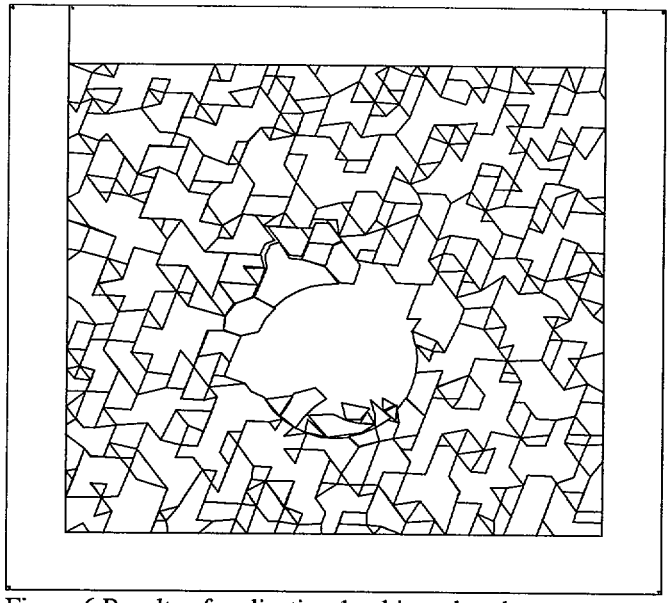

Figure 6 Results of realization 1 subjected to the acceleration time history shown in Figure 3 with a 2/5 scaling to the amplitude

the one shown in Figure 3 with no amplitude scaling. Compare the extent of rockfall in this figure with that in Figure 4(a), where the amplitude was scaled by a factor of 1/5, it is clear that the excavation subjected to a larger magnitude of ground motion (Fig. 5) suffers much more damage than the excavation subjected to a smaller ground motion [Fig. 4(a)]. This observation is consistent with the field observations reported elsewhere (Sharma and Judd, 1991, Hsiung et al. 1992); an indication that the DDA performs reasonably well in capturing the responses of excavations to ground motions. However, it should be noted that the extent of damage or whether or not higher magnitudes of earthquakes will cause more damage depends greatly on rock block geometries. While higher magnitudes of ground motions cause more damage to realization 1 as shown in Figures 5 and 4(a), the extent of damage is essentially the same for realization 3.

Compared with the case in Figure 4(a), additional rockfall was not observed until the amplitudes with a scaling factor of ½ to the amplitudes were used. Figure 6 shows the results of rockfall for realization 1 with a 2/5 scaling. The extent of rockfall in Figure 6 is the same as that observed in Figure 4(a). However, a slightly more movements for blocks located at the top right side of the excavation can be observed for the case in Figure 6 than in Figure 4(a). These movements are primarily related to joint shear and normal displacements. The extent of rockfall for the case with a ½ scaling as shown in Figure 7 is comparable to that observed in a case with no scaling applied.

Dynamic analysis on response of rock media in time domain is a complex matter. The technology available for such analysis is fairly recent. Consequently, the effects of the characteristics of seismic signals on the behavior of joint rock media are not well understood. The problem is further complicated by the fact that time domain ground motion data in the areas of interest are often not available. On occasion harmonic-based time history with one dominant frequency is used as a substitute. The appropriateness of adopting this approach has not been addressed adequately. This issue will be addressed in a separate paper.

Figure 8 shows the responses of realization 1 after the second episode of earthquake under different ground motions. The amplitudes of the input acceleration time histories were 1/5 scale of Figure 3. The response to the first earthquake for the same realization is shown in Figure 4(a). The seismic signals used were the same for both the first and second earthquakes. Additional damage can be observed after the second ground motion [Fig. 8 versus Fig. 4(a)]; significantly more rockfall took place to actually fill up the entire excavation. The result demonstrates that repeated ground motions could have a detrimental effect on excavation stability. Upon close examination of Figure 4(a), one can find accumulation of joint deformation at the top left side of the excavation after the first earthquake. This accumulation weakened the rock mass considerably even though the excavation remained stable. During the second episode of ground motion, additional joint deformation accumulated in the same region and eventually triggered rockfall because the

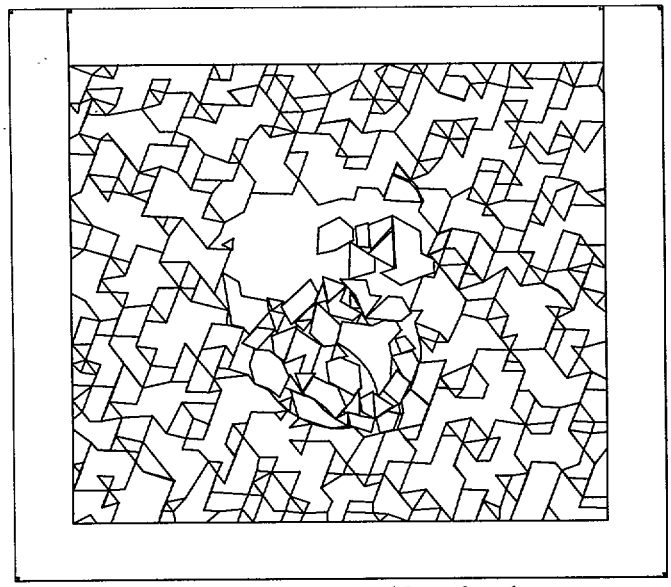

Figure 7 Results of realization 1 subjected to the acceleration time history shown in Figure 3 with a ½ scaling to the amplitude

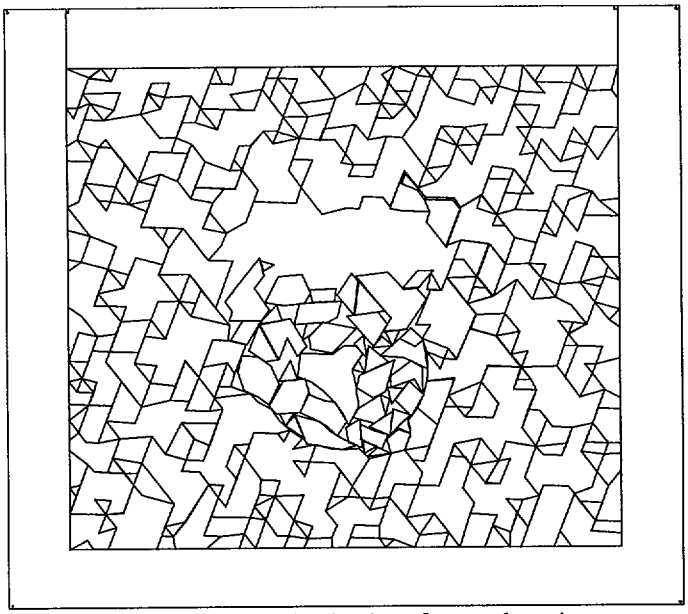

Figure 8 Effect of repeated episodes of ground motions on underground excavation stability for realization 1, after two episodes of earthquakes with two identical input time histories. The time history used is same as that for Figure 4(a)

remaining joint strength could no longer hold the rock blocks in place (Fig. 8). This finding confirms further the observations both in the laboratory and field that seismic events are likely to influence stability through accumulation of permanent deformations around underground excavations (Brown and Hudson, 1974, Barton and Hansteen, 1979, Hsiung et al. 1999). This finding also supports the notion that the fundamental failure mechanism for an excavation in a jointed rock medium subjected to repeated episodes of seismic events is accumulation of joint deformations (Hsiung et al., 1992, 1999).

The DDA results presented so far in this paper are based on the 1st order polynomial displacement function. Under this approximation, the strains in each block are constant. This 1st order approximation is equivalent to a triangular element in FEM. Hsiung (2001) extended the DDA code to include a user option of selecting polynomial displacement function of any order at run time. The 1st and 2nd order displacement functions were used for a DDA block model to examine the difference in results. The 2nd order function in the DDA is equivalent to a shape function for the four-noded element in FEM except that the latter lacks x^2 and y^2 terms. Figure 9 indicates that the 2nd order polynomials resulted in an excavation [Fig. 9(b)] that was more stable than that of the 1st order polynomials [Fig. 9(a)]. Figure 9(a) shows that shear displacements and separations of joints in rocks at the top right side of excavation were more pronounced than those in Figure 9(b). This behavior is reasonable because DDA blocks are stiffer for the 1st order polynomial displacement function that those for the 2nd order approximation. As a result, blocks with the 2nd order approximation deform more; thus the energy available for joint to slip is reduced. Consequently, joint deformation will be less.

5 CONCLUSIONS

The DDA was used to analyze dynamic response of underground excavation. The results indicate that DDA is suitable for assessing performance of underground excavations subjected to ground motions where joint parameter uncertainties is expressed as probability distribution. Incorporation of parameter uncertainties in the DDA will be useful in the design of underground excavations in earthquake-prone regions. Specific findings of the study include that:

- the extent of rockfall depends highly on block geometries surrounding excavations;
- repeated episodes of ground motions could potentially cause additional damage to underground excavations; and
- relatively less damage is predicted for an underground excavation if the 2nd order polynomial displacement function is used instead of the 1st order.

DDA results confirm the observation that instability of underground excavations is a result of progressive accumulation of joint deformation.

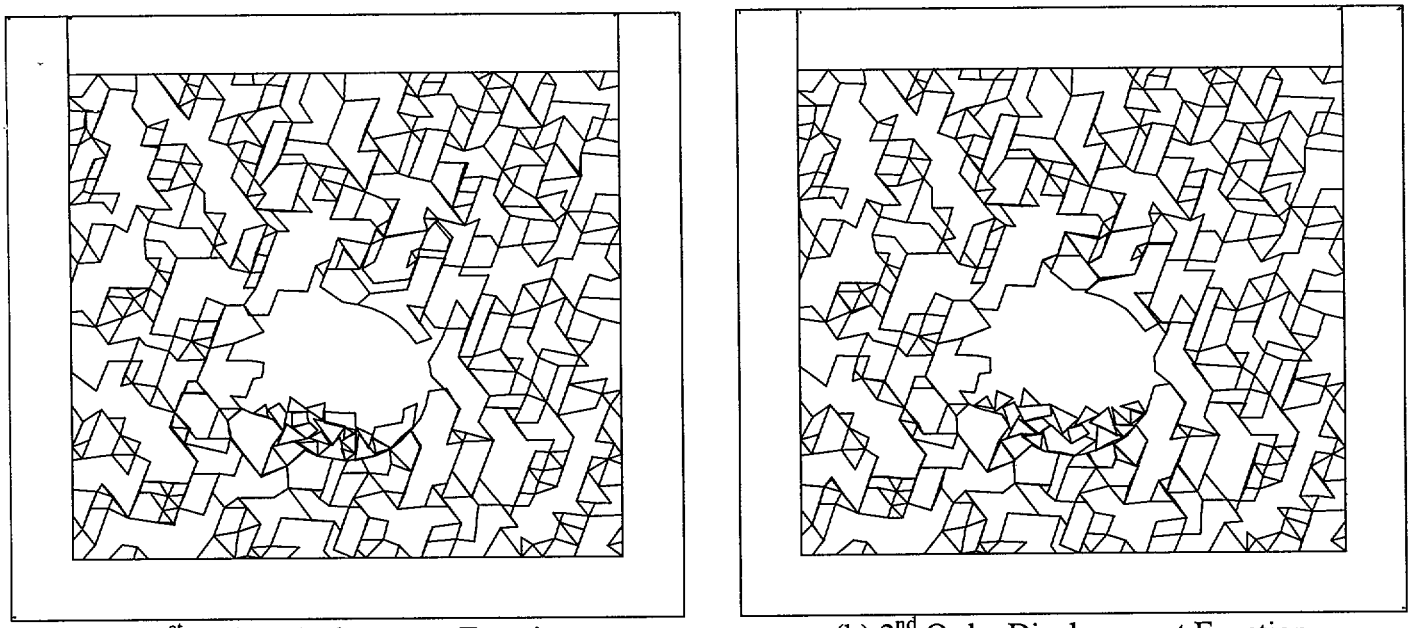

(a) 1st Order Displacement Function

(b) 2nd Order Displacement Function

Figure 9 Effects of order of displacement functions

ACKNOWLEDGMENTS

This abstract documents work performed by the Center for Nuclear Waste Regulatory Analyses (CNWRA) on behalf of the Nuclear Regulatory Commission (NRC) Office of Nuclear Material Safety and Safeguards, Division of Waste Management. This work is an independent product of the CNWRA and does not necessarily reflect the views or regulatory position of the NRC.

REFERENCES

Barton, N., and H. Hansteen. 1979. Very large span openings at shallow depth: Deformation magnitudes from jointed models and finite element analysis, *Proceedings of the Fourth Rapid Excavation and Tunneling Conference* 2: 1,331-1,353.

Brown, E.T., and J.A. Hudson. 1974. Fatigue failure characteristics of some models of jointed rock, *Earthquake Engineering and Structural Dynamics* 2: 379-386.

Hsiung, S.M., W. Blake, A.H. Chowdhury, and T.J. Williams. 1992. Effects of Mining-Induced Seismic Events on a Deep Underground Mine, *PAGEOPH*, 139(3/4), 741-762.

Hsiung, S.M., J.D. Fox, and A.H. Chowdhury. 1999. Effects of Repetitive Seismic Loads on Under-ground Excavations in Jointed Rock Mass, *Radioactive Waste Management and Environ-mental Remediation – ASME*, 622.

Hsiung, S.M. 2001. Discontinuous Deformation Analysis (DDA) With n^{th} Order Polynomial Displacement Functions, Submitted to the *38th U.S. Rock Mechanics Symposium*, July 7-10, 2001, Washington, DC.

Kana, D.D., B.G.H. Brady, B.W. Vanzant, and P.K. Nair. 1989. *Critical Assessment of Seismic and Geomechanics Literature Related to a High-Level Nuclear Waste Underground Repository*, NUREG/CR-5440, Center for Nuclear Waste Regulatory Analyses, San Antonio, TX.

Law, H.K., and I.P. Lam. 1999. Application of Key Block Theory and DDA at Yerba Buena Island Tunnel Portals Under Earthquake Loading, *Proceedings of the Third International Conference on Analysis of Discontinuous Deformation*, 181-190, B. Amadei ed. American Rock Mechanics Association, Alexandria, VA.

Sharma, S., and W.R. Judd. 1991. Underground opening damage from earthquakes, *Engineering Geology*, 30, 263-276.

Shi, G.H. 1996. Discontinuous Deformation Analysis – Technical Note, *First International Forum on Discontinuous Deformation Analysis*, June 12-14, 1996, Berkeley, CA.

Shi, G.H. 1999. Applications of Discontinuous Deformation Analysis and Manifold Method, *Proceedings of the Third International Conference on Analysis of Discontinuous Deformation*, 3-15, B. Amadei ed. American Rock Mechanics Association, Alexandria, VA.

Wu, Y-T., H.R. Millwater, and T.A.Cruse. 1990. Advanced Probabilistic Structural Analysis Method for Implicit Performance Functions, *AIAA Journal*, 28(9), 1663-1669.

Discontinuous Deformation Analysis (DDA) with n^{th} order polynomial displacement functions

S.M. Hsiung
Center for Nuclear Waste Regulatory Analyses, Southwest Research Institute

ABSTRACT: Discontinuous Deformation Analysis (DDA) is a technique suitable for investigating fractured rock-mass behavior and geotechnical and structural problems. In the initial implementation of DDA, the 1st order polynomial displacement function was used to approximate the movement of any point in a two-dimensional (2D) domain. As a result, the stress and strain within a block in the model were constant. This study presents the results of an effort to develop a more general approach in which the DDA is implemented with higher order polynomial displacement functions. The higher order displacement functions make accurate modeling of complicated stress and strain fields in blocks possible.

1 INTRODUCTION

Discontinuous Deformation Analysis (DDA) is suited to investigating fractured rock-mass behavior important to many geotechnical and structural problems. DDA method is the block system version of the finite element method (FEM). It involves a finite element type of mesh where all elements are real isolated blocks, bounded by pre-existing discontinuities (or joints). Although DDA method seems to resemble the distinct element method in that it accounts for joint contact behavior, mathematically it parallels FEM in the following aspects (Shi, 1996)

- DDA establishes its equilibrium equations by minimizing the total potential energy of the system;
- DDA uses displacements as unknowns for the simultaneous equations; and
- Stiffness, mass, and loading matrices of individual blocks are calculated independently and added to the global matrix of the entire system.

The blocks simulated in the DDA method can be of any shape (both convex and concave). An implicit solution algorithm is adopted in the DDA. The large displacements of the blocks are accounted for by the use of a time step scheme; at the end of each time step, the equilibrium is reached by minimizing the total potential energy, and block geometry is updated. The deformed block geometry and the resulting state of stresses from the previous time step is used as the initial condition for the next time step.

In the original DDA formulation (Shi, 1993, 1996), it was suggested that a polynomial displacement function could be used to describe the movement of any point in a two-dimensional (2D) domain. In developing the computer code for DDA, a 1st order polynomial displacement function was assumed, so that the stresses and strains within a block in the model were constant. This approximation precludes the application of the 1st order polynomial function to problems with significant stress variations within the block.

An approach to resolve this problem was to glue small blocks together to form a larger block. This approach results in a penalty in computing time. Some researchers (Chang, 1994, Clatworthy and Scheele, 1999) added finite element meshes in the blocks so that stress variations within the blocks can be accounted for. While this approach works adequately, the extent of stress variation that can be accounted for depends on the number of finite elements included in a block. An alternative approach is to include more polynomial terms in the displacement function. For example, Chern et al. (1995) added the second order. Ma et al. (1997) and Koo and Chern (1997) implemented the third order displacement function in the DDA method. The results show an improvement in accuracy of calculated stresses and displacements.

However, these approaches did not take full advantage of the original formulation, which allows for implementation of a polynomial displacement function of any order. Furthermore, there are applications that may require using polynomials greater than the third order to achieve better accuracy or more efficiency in calculation by reducing the total degree of freedom for the problem. For example, using the 3rd order displacement function, Ma et al. (1997) found that despite the improvement in obtaining accurate results the calculated vertical displacement at the free end of a cantilever beam was still substantially smaller than the theoretical solution. Koo and Chern (1997) found that a much closer solution could be achieved by using 32 blocks to represent the beam. These observations suggest that even higher order polynomials may be necessary for certain problems. Toward this end, an effort was made to develop a more general formulation of the DDA that will accept any order of polynomial displacement function.

2 DISPLACEMENT FUNCTION

As discussed in the previous section, in DDA, the large displacements are an accumulation of the small displacements and deformations in a time step. Within each time step, the x- and y-direction displacements, *(u,v)*, at any point *(x,y)* in a block can be represented using the approximation of an n-order polynomial displacement function:

$$u = \sum_{\ell=0}^{n}\sum_{m=0}^{\ell} d_{2(m+\sum_{k=1}^{\ell}k)+1}\, x^{\ell-m}y^{m}$$
$$v = \sum_{\ell=0}^{n}\sum_{m=0}^{\ell} d_{2(m+\sum_{k=1}^{\ell}k)+2}\, x^{\ell-m}y^{m} \qquad (1)$$

where n is the order, ℓ is an integer from 0 to n, m is an integer from 0 to ℓ, and d_j are the coefficients of the polynomial function. Eq. (1) can be expressed as:

$$\begin{pmatrix} u \\ v \end{pmatrix} = [W_i]_{2\times(\sum_{\ell=1}^{n+1}2\ell)}\,[D_i]_{(\sum_{\ell=1}^{n+1}2\ell)\times 1} \qquad (2)$$

where the subscript i represents the ith block; $[W_i]$, called transformation function in this paper, are a collection of the $x^{\ell-m}y^{m}$ terms in Eq. (1) and a $2\times\sum_{\ell=1}^{n+1}2\ell$ matrix; and $[D_i]$ are the collection of coefficients of the polynomial displacement function, d_j, and a $\sum_{\ell=1}^{n+1}2\ell\times 1$ matrix.

3 DDA FORMULATION FOR THE n[th] ORDER DISPLACEMENT FUNCTION

Assuming that a system contains N number of blocks, the total potential energy Π_s of the system has the form

$$\Pi_s = \frac{1}{2}[D_s]^T[K_s][D_s] + [D_s]^T[F_s] + C \qquad (3)$$

where $[D_s]^T = \begin{bmatrix} D_1^T & D_2^T & \cdots & D_N^T \end{bmatrix}$ is a matrix containing displacement variables of the system; $[F_s]^T = \begin{bmatrix} F_1^T & F_2^T & \cdots & F_N^T \end{bmatrix}$ is the system force matrix;

$$[K_s] = \begin{bmatrix} K_{11} & K_{12} & \cdots & K_{1N} \\ K_{21} & K_{22} & \cdots & K_{2N} \\ \vdots & \vdots & \ddots & \vdots \\ K_{N1} & \cdots & \cdots & K_{NN} \end{bmatrix}$$ is the system stiffness matrix (Shi, 1996); and C is the energy produced by friction force. If an n order displacement function is chosen, there are $\sum_{\ell=1}^{n+1}2\ell$ displacement variables/unknowns for each block. As a result, each element in $[D_s]$ and $[F_s]$ is a $1\times\sum_{\ell=1}^{n+1}2\ell$ matrix and each element in $[K_s]$ is a $\sum_{\ell=1}^{n+1}2\ell\times\sum_{\ell=1}^{n+1}2\ell$ matrix.

By minimizing the total potential energy of the system, a set of simultaneous equations can be obtained

$$[K_s][D_s] = [F_s] \qquad (4)$$

The stiffness matrix $[K_s]$ and the force matrix $[F_s]$ take the contribution from the elastic strains, displacement and load boundary conditions, initial stresses, force of inertia, and contacts between blocks. The general forms of the formulations for these contributions for the n[th] order approximation are similar to those for the 1st order approximation except that appropriate transformation functions should be used. For a detailed discussion on the formulations for the 1st order approximation, readers should refer to Shi (1993, 1996). In this paper, formulations for block stiffness, initial stresses, body force, and distributed load are provided.

3.1 *Block Stiffness Matrix*

The strain energy Π_e for block i is

$$\Pi_e = \iint \frac{1}{2}[\varepsilon_i][\sigma_i]\,dxdy \qquad (5)$$

where $[\sigma_i]$ is the stress matrix and $[\varepsilon_i]$ is the strain matrix of block i. The stress-strain relationship can be presented as

$$[\sigma_i] = [E_i][\varepsilon_i] \tag{6}$$

For a plane stress condition

$$[E_i] = \frac{E}{1-\nu}\begin{bmatrix} 1 & \nu & 0 \\ \nu & 1 & 0 \\ 0 & 0 & \frac{1-\nu}{2} \end{bmatrix} \tag{7}$$

where E and ν are Young's modulus and Poisson's ratio, respectively; and the strains $[\varepsilon_i]$ can be determined by

$$\begin{bmatrix} \varepsilon_x \\ \varepsilon_y \\ \gamma_{xy} \end{bmatrix} = \begin{bmatrix} \frac{\partial u}{\partial x} \\ \frac{\partial v}{\partial y} \\ \frac{\partial u}{\partial y} + \frac{\partial v}{\partial x} \end{bmatrix} = [B_i][D_i] \tag{8}$$

The $[B_i]$ matrix can be obtained by taking the derivative of the elements in $[W_i]$ with respect to appropriate variables indicated in Eq. (8).

Substituting Eqs. (6) and (8) into Eq. (5), the strain energy of block i can be expressed as

$$\Pi_e = \iint \frac{1}{2}[D_i]^T[B_i]^T[E_i][B_i][D_i]\,dxdy \tag{9}$$

The contribution of the stiffness matrix to the overall stiffness matrix for block i is computed by minimizing Eq. (9)

$$[K_{ii}] = \iint [B_i]^T[E_i][B_i]\,dxdy \tag{10}$$

It should be noted that the elements in $[B_i]$ matrix contain $x^{n_1}y^{n_2}$ terms, where n_1 and n_2 are integers equal to or greater than 0. Consequently, integration for Eq. (10) is not straightforward. The higher the order for the polynomial function, the more difficult it is to integrate. Shi (1994) presented the analytical solutions that make integration of any polynomial term possible; thus making the development of a generalized procedure for selecting the order of displacement function at run time possible. Chen and Ohnishi (1999) further reduced the solutions to a more manageable form. This development work adopted the formulas proposed by Chen and Ohnishi (1999).

3.2 *Initial Stress*

The initial stresses $[\sigma_i^0]$ in block i for a previous time step are

$$[\sigma_i^0] = [E_i][\varepsilon_i^0] = [E_i][B_i][D_i^0] \tag{11}$$

The potential energy Π_{σ^0} for the initial stresses in block i can be expressed as

$$\begin{aligned} \Pi_{\sigma^0} &= \iint [\varepsilon_i][\sigma_i^0]\,dxdy \\ &= \iint [D_i]^T[B_i]^T[E_i][B_i][D_i^0]\,dxdy \end{aligned} \tag{12}$$

The contribution of the initial stresses in block i to the overall force matrix is calculated by minimizing Eq. (12)

$$[F_i] = -\iint [B_i]^T[E_i][B_i]\,dxdy\,[D_i^0] \tag{13}$$

3.3 *Body Force*

The potential energy of a constant body force $[f_x \quad f_y]$ for the ith block is

$$\Pi_B = -\iint [u \quad v]\begin{bmatrix} f_x \\ f_y \end{bmatrix} dxdy \tag{14}$$

Substituting Eq. (2) into Eq. (14), the potential energy equation can be rewritten as

$$\Pi_B = -\iint [D_i]^T[W_i]^T\begin{bmatrix} f_x \\ f_y \end{bmatrix} dxdy \tag{15}$$

Minimizing Eq. (15), the contribution of the body force in block i to the overall force matrix is

$$[F_i] = \iint [W_i]^T dxdy \begin{bmatrix} f_x \\ f_y \end{bmatrix} \tag{16}$$

3.3 *Distributed Load*

Assuming that a distributed load acts on a straight line from point $P_1(x_1, y_1)$ to $P_3(x_3, y_3)$, a point (x, y) on the line segment $\overline{P_1P_3}$ is

$$\begin{aligned} x &= x_2 t + x_1 \\ y &= y_2 t + y_1, \qquad 0 \le t \le 1 \end{aligned} \tag{17}$$

where $x_2 = x_3 - x_1$ and $y_2 = y_3 - y_1$.

The length ℓ of $\overline{P_1P_3}$ is

$$\ell = \sqrt{x_2^2 + y_2^2} \tag{18}$$

Assuming that the distributed load is a function of t and can be expressed as

$$\begin{aligned} F_x &= F_x(t) \\ F_y &= F_y(t), \qquad 0 \le t \le 1 \end{aligned} \tag{19}$$

The potential energy Π_d of the distributed load is

$$\begin{aligned} \Pi_d &= -\int_0^1 [u \quad v]\begin{bmatrix} F_x(t) \\ F_y(t) \end{bmatrix} \ell\,dt \\ &= -[D_i]^T \int_0^1 [W_i]^T \begin{bmatrix} F_x(t) \\ F_y(t) \end{bmatrix} \ell\,dt \end{aligned} \tag{20}$$

The contribution of the distributed load to the overall force matrix, by minimizing Eq. (20), is

$$[F_i] = \ell \int_0^1 [W_i]^T \begin{bmatrix} F_x(t) \\ F_y(t) \end{bmatrix} dt \quad (21)$$

When the distributed load is a constant, that is, $[F_x(t) \quad F_y(t)] = [F_x \quad F_y]$, Eq. (21) can be shown as

$$[F_i] = \left(\int_0^1 [W_i]^T dt \right) \ell \begin{bmatrix} F_x \\ F_y \end{bmatrix} \quad (22)$$

The matrix integration of Eq. (22) has an analytical solution. For any polynomial term $x^{n_1} y^{n_2}$ in the transformation function $[W_i]$, the integration can be performed

$$\int_0^1 x^{n_1} y^{n_2} dt = \int_0^1 (x_2 t + x_1)^{n_1} (y_2 t + y_1)^{n_2} dt \quad (23)$$

Integrating Eq. (23), one can obtain

$$\int_0^1 x^{n_1} y^{n_2} dt = \sum_{k_1=0}^{n_1} \sum_{k_2=0}^{n_2} a \binom{n_1}{k_1} \binom{n_2}{k_2} x_1^{n_1-k_1} x_2^{k_1} y_1^{n_2-k_2} y_2^{k_2}, \quad n_1 > 0 \text{ and } n_2 > 0 \quad (24)$$

where $\binom{n_1}{k_1}$ and $\binom{n_2}{k_2}$ are binomial coefficients and $a = \dfrac{1}{n_1 + n_2 - k_1 - k_2}$.

If the applied distributed load is linearly varying from $(F_x \quad F_y)$ at P_1 to $(F_{x_3} \quad F_{y_3})$ at P_3, this applied load can be divided into two parts. The first part is a constant distributed load with which Eq. (24) can be used to compute the contribution. The second part is a distributed load varying from 0 at P_1 to $(F_{x_3} - F_x \quad F_{y_3} - F_y)$ at P_3 and the force contribution is

$$[F_i] = \ell \int_0^1 [W_i]^T \begin{bmatrix} t(F_{x_3} - F_x) \\ t(F_{y_3} - F_y) \end{bmatrix} dt = \ell \begin{bmatrix} F_{x_3} - F_x \\ F_{y_3} - F_y \end{bmatrix} \int_0^1 t\,[W_i]^T dt \quad (25)$$

Integration of any polynomial term $x^{n_1} y^{n_2}$ in the transformation function $[W_i]$ for Eq. (25) will yield

$$\int_0^1 t x^{n_1} y^{n_2} dt = \sum_{k_1=0}^{n_1} \sum_{k_2=0}^{n_2} a_1 \binom{n_1}{k_1} \binom{n_2}{k_2} x_1^{n_1-k_1} x_2^{k_1} y_1^{n_2-k_2} y_2^{k_2}, \quad n_1 > 0 \text{ and } n_2 > 0 \quad (26)$$

where $a_1 = \dfrac{1}{n_1 + n_2 - k_1 - k_2 + 2}$.

4 VERIFICATION OF MODIFIED DDA CODE

This research work extended the original DDA to permit options of selecting an appropriate order of polynomial displacement function compatible with the displacement fields in a system. Several problems were chosen to verify the modified code (DDA-CT2.0) with the focus on examination of the performance of a single block. These problems were related to behavior of a single beam under various loading conditions.

4.1 *Beam Subjected to Axial Load*

Figure 1 shows a beam subjected to an axial load at its free end. The length of the beam, load magnitude [1.0 ton (T)], and material properties of the beam are provided in the figure. The height of the beam is 1 m.

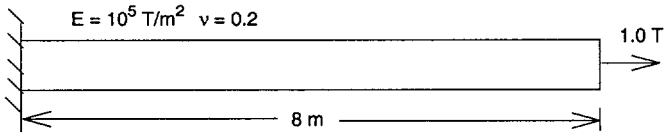

Figure 1. Beam subjected to axial load

The axial deformation along the axis of a beam subjected to an axial load is

$$\Delta = \frac{Px}{AE} \quad (28)$$

where Δ is the axial deformation, x is the distance from the fix end, A is the cross-sectional area, and E is the Young's modulus of the beam. P in Eq. (28) can be a concentrated load acting at the middle point of the free end or is equal to $p\ell$ if a distributed load is applied. p denotes the distributed load and ℓ is the height of the beam.

The DDA modeling results and the theoretical solutions along the axis of the beam are presented in Figure 2. It can be seen from the figure that the DDA modeling with one block does not give accurate results until a polynomial displacement function having an order greater than or equal to 3 is used for a distributed load.

Similar observation can be made for a concentrated load. The DDA using the 3rd order displacement function gives results that are identical to the theoretical solutions for a concentrated load. However, the DDA prediction starts to deviate from the theoretical solutions when the displacement functions with an order greater than 4 are used for displacement approximation. As can be observed in Figure 2, deformations at the free end are overestimated for the 5th and 10th order of

displacement function approximations for the case of a concentrated load. This behavior is explainable because blocks become less stiffer when higher order displacement functions are used; thus permit highly localized deformation in a block, particularly in areas surrounding the applied loads. The localized deformations are more pronounced for concentrated loads than those for distributed loads. Further studies indicate that, depending on the magnitude of the load applied, the localized deformation for a beam subjected to an axial load becomes noticeable when using a displacement function of an order greater than 9 with a distributed load or greater than 4 with a concentrated load.

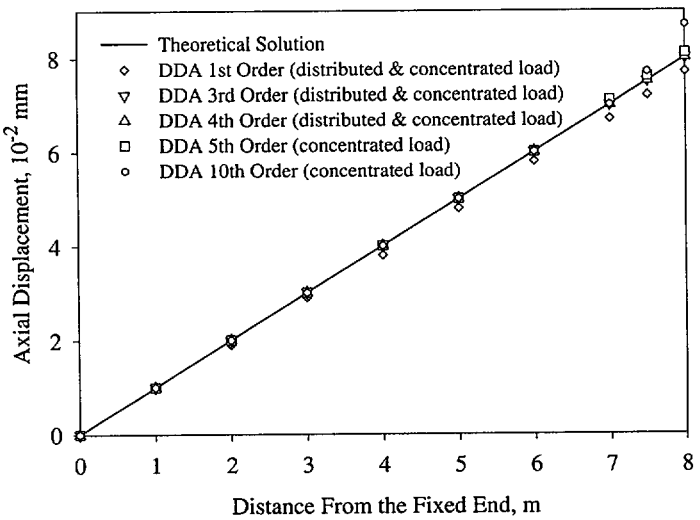

Figure 2. DDA modeling results for beam subject to axial load

4.2 *Cantilever Beam*

The second verification problem is related to a cantilever beam subjected to a concentrated load perpendicular to the beam axis at the free end. The length and material properties of the beam, and the magnitude of the applied load are provided in Figure 3. The beam is 1-m high.

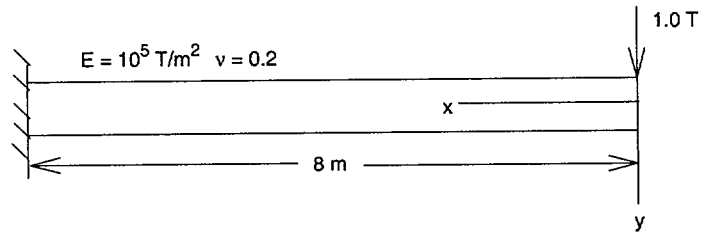

Figure 3. Cantilever beam

The approximate deflection $v_{y=0}$ of the axis of the cantilever is

$$v_{y=0} = \frac{P}{6EI}\left(2L^3 - 3L^2x + x^3\right) \qquad (29)$$

where L is the length of the beam and I is the moment of inertia of the cross section of the cantilever. The deflection of the cantilever axis calculated using Eq. (29) is plotted in Figure 4 and labeled as theoretical solution.

Figure 4 shows the results of DDA modeling of a cantilever beam. As can be observed, the 1st order approximation for the displacements in blocks is not suitable for modeling bending related problems. The modeling results are improved substantially when the 2nd order polynomials are used. The calculated deflection at the free end is about 72.97% of the theoretical value. The calculated result is improved further the 3rd order polynomials are used; the calculated deflection at the free end is about 97.91% of the theoretical value. It is worthwhile noting that the results using the 3rd order polynomials presented in this paper are significantly different from those presented by Ma et al. (1997) and Koo and Chern (1997). The study performed by Ma et al. (1997) used just one block as did in this study and the predicted deflection of the cantilever axis was substantially smaller than the theoretical solutions. Koo and Chern (1997) used 32 blocks to model a cantilever beam for their study to bring the predicted deflections closer to the theoretical values. It would appear that the results presented in this paper are more reasonable because the vertical displacement at the free end of a cantilever beam is a function of beam length to the third power.

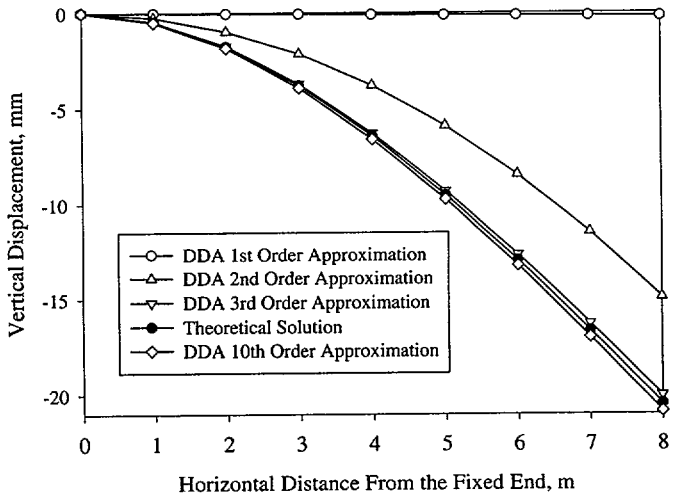

Figure. 4 DDA modeling results on deflection of a cantilever beam

The DDA modeling using the 10th order polynomials produces a deflection at the free end of the cantilever larger than that of the theoretical solution (Figure 4); the calculated value is about 101.91% the theoretical value. It should be noted that the theoretical solutions provided by Eq. (29) represent a reasonable approximation of the behavior of a cantilever. This equation neglects the potential effects of the shear deformations. The latter deformations are usually very small, if beam

length is substantially larger than beam height (Popov, 1970, Timoshenko and Goodier, 1987). The shear deformation at the free end of a cantilever is

$$v_{y=0,\,shear} = \frac{6PL}{5AG} \tag{30}$$

where A is the cross-sectional area and G is the shear modulus of the beam. By including this shearing deformation in the theoretical solution for the free end, the DDA result is about 100.78% of the theoretical value. The remaining overestimation may be attributed to the approximation of curvature $1/\rho$ used to develop beam theory.

4.3 *Simply Supported Beam*

Figure 5 illustrates a simply supported beam with specifics on beam length, material properties, and the load applied. The height of the beam is 1 m. A concentrated load of 100 ton was applied to the middle span of the beam.

The deflection of the beam axis for this case is

$$v_{y=0} = -\frac{Px}{48EI}\left(3L^2 - 4x^2\right), \quad 0 \le x \le \frac{L}{2} \tag{33}$$

The deflection of axis for the simply supported beam computed from Eq. (33) is presented in Figure 6.

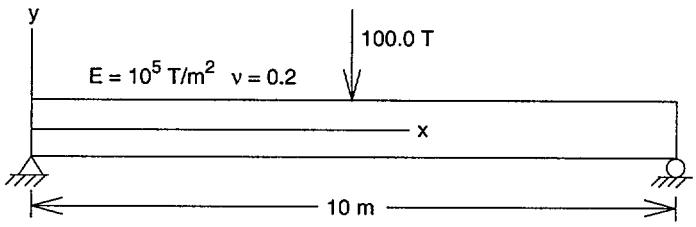

Figure 5. Simply supported beam

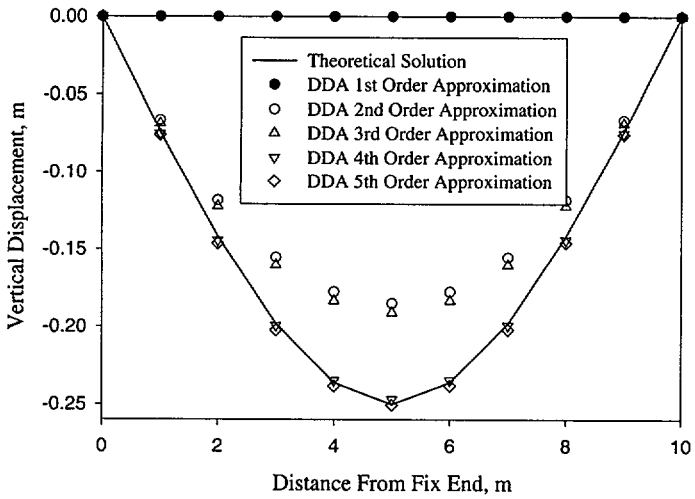

Figure 6 DDA results for simply supported beam

Also shown in the figure are DDA results using the 1st, 2nd, 3rd, 4th, and 5th order polynomial displacement functions. It can be observed that significant improvement can be made to model a simply supported beam by replacing the original 1st order polynomial displacement function with the 2nd order approximation. Use of the 3rd order function improves the results only slightly as compared to the 2nd order polynomials. The DDA modeling using the 4th or 5th order displacement function gives much more precise prediction results. The predicted deflection at the middle span of the beam is 98.72% and 100.22% of the theoretical value for the 4th and 5th order polynomials, respectively.

4.4 *Buckling of a Beam*

In the structural engineering field, the elastic stability, or the sidewise buckling of compressive members, is of great practical importance. In this study, a long, perfectly straight (ideal) beam built-in at one end and free at the other as shown in Figure 7 was modeled to assess the ability of DDA in simulating beam buckling problems. As shown in Figure 7, a beam is subjected to both an axial compressive force and a lateral force at the free end. The applied lateral force is pointed downward and is 1.0 T in most of the cases. The length and material properties of the beam are also given in the figure. The height of the beam is 1 m.

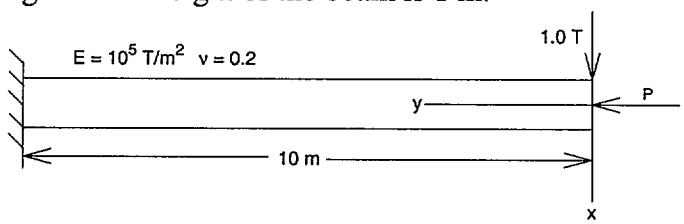

Figure 7 DDA Buckling model

The beam is modeled in DDA as a weightless block. The modeling procedure follows three distinct steps. The first step is to apply the axial compressive force; followed by adding and then removing the lateral force. At each step, an equilibrium condition is reached before the subsequent step is implemented.

For the beam considered in Figure 7, a buckling condition exists if the applied axial compressive force at the free end exceeds the critical load P_{cr}. P_{cr} can be determined using the Euler formula as shown in Eq. (34) (Popov, 1970, Timoshenko, 1956)

$$P_{cr} = \frac{\pi^2 EI}{4\ell^2} \tag{34}$$

This critical load is also called Euler load. When the critical load P_{cr} is reached or surpassed, a small lateral force applied at the side of the free end may produce large lateral deflections. These deflections

are not recoverable after this lateral force is removed. Using the dimension and material properties provided in Figure 7, Eq. (34) gives a critical load of about 205.62 T.

Figure 8 provides the relationship between the applied axial compressive forces and the resulting non-recoverable lateral deflections at the free end calculated from the DDA results for the 3rd, 4th, and 5th displacement functions. The horizontal line in the figure denotes a zero deflection state indicating that the beam is in a straight position. The positive deflection indicates that the beam is deflected in the same direction as the lateral force while the negative deflection means that the deflection is in a direction opposite to that of the applied lateral force. In other words, relative to the beam in Figure 7, the deflections for the downward buckling are positive and they are negative if the beam buckled upward.

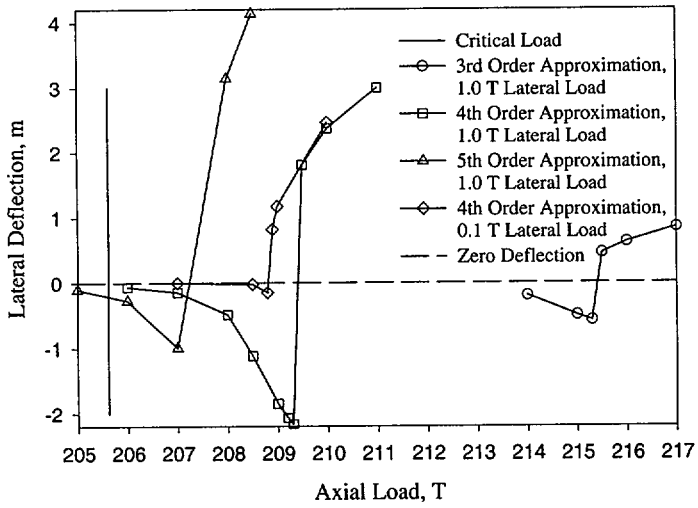

Figure 8 DDA results for buckling simulation

The DDA results as shown in Figure 8 seem to suggest that a beam subjected to an axial compressive force and a small downward (lateral) force could buckle either downward (direction of the lateral force) or upward (opposite direction of the lateral force) irrespective of the displacement functions used. Figure 9 shows the locus of the movement of the free end as a function of time steps for a typical upward buckling. It can be seen that, after removal of the lateral force, the beam buckled eventually to the opposite side when a state of neutral equilibrium was reached.

The transitional axial compressive force at which the direction of the buckling changes from upward to downward is difficult to determine. This is especially the case for higher order displacement functions because a very large number of time steps (cycles) are needed for displacement of the beam to reach equilibrium after the applied lateral force is removed. At or near the transitional axial force, the deflection for the upward buckling is the largest, and as the axial force becomes smaller such deflection diminishes. Likewise (in a similar manner), the deflections associated with the downward buckling increase along with an increase in the applied axial force.

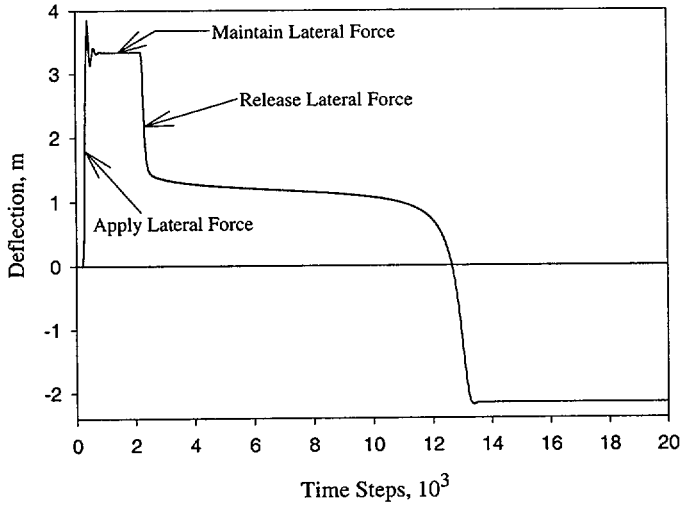

Figure 9 Displacement of the free end of the cantilever as a function of time steps subjected to 209.3 T axial and 1.0 T lateral forces using the 5th order displacement function

It is interesting to note that the range of the axial compressive force within which the non-recoverable upward deflection exists is quite narrow; for example, this range is approximately between 206 and 209.3 T if the 4th polynomial displacement function is used. Although the DDA results suggest that a buckling at the opposite direction of the applied lateral force may exist, it is not clear if such buckling is physically plausible or simply an artifact of modeling. The DDA results further suggest that such buckling phenomena will disappear if a much smaller lateral force is used to disturb the equilibrium. Figure 8 also includes a curve representing non-recoverable deflections for cases where a lateral force of 0.1 T is applied and removed. This curve was developed using the 4th order polynomials. Negligible buckling at the opposite direction is observed.

As discussed earlier, it is not known if a buckling in the opposite direction of the applied lateral force is feasible. Consequently, only the buckling in the direction of the lateral force is assumed to be possible. Based on this assumption, the results presented in Figure 8 for the three displacement functions indicate that DDA results tend to overestimate the critical load (about 205.62 T for the theoretical value) for buckling to occur. Among them, the 5th order displacement function produces a better result.

5 CONCLUDING REMARKS

A generalized procedure was developed to permit selection of the order of the polynomial displacement functions suitable for the nature of the applications in hand by modelers. In this study, several beam problems under various loading conditions were used to assess the effectiveness of the generalized procedure. The results indicate that the procedure has been correctly implemented. The study also found that displacement functions with 4^{th} or 5^{th} order are sufficient to model most of the beam behavior using one block.

The success of implementing this procedure is expected to expand the potential applications of DDA to areas where estimation of more accurate stresses and deformations is needed, for example, crack propagation. This procedure can be developed further via minor modifications so that each block or a group of blocks in a system can be to be modeled with different orders of displacement functions. This expansion will be beneficial to permit focusing studies in areas of interest of an application while maintaining the necessary efficiency of the modeling.

ACKNOWLEDGMENT

This paper documents work performed by the Center for Nuclear Waste Regulatory Analyses (CNWRA) on behalf of the Nuclear Regulatory Commission (NRC) Office of Nuclear Material Safety and Safeguards, Division of Waste Management. This work is an independent product of the CNWRA and does not necessarily reflect the views or regulatory position of the NRC. The author thanks Dr. G.H. Shi for his guidance and inspiration.

REFERENCES

Chang, T.C., *Nonlinear Dynamic Discontinuous Deformation Analysis with Finite Element Meshed Block System*, Ph.D. Dissertation, Department of Civil Engineering, University of California, Berkeley, California, 1994.

Chen, G., and Y. Ohnishi, Practical Computing Formulas of Simplex Integration, *Proceedings of the 3rd International Conference on Analysis of Discontinuous Deformation from Theory to Practice*, Ed., B. Amadei, 75-84, Vail, CO, 1999.

Chern, J.C., Koo, C.Y., and S. Chen, Development of Second Order Displacement Function for DDA and Manifold Method, *Working Forum on the Manifold Method of Material Analysis*, Vol. 1, 183-202, U.S. Army Corps of Engineers, Waterways Experiment Station, Vicksburg, MS, 1995.

Clatworthy, D., and F. Scheele, A Method of Sub-Meshing in Discontinuous Deformation, *Proceedings of the 3rd International Conference on Analysis of Discontinuous Deformation from Theory to Practice*, B. Amadei, Ed., 85-94, Vail, CO, 1999.

Koo, C.Y., and J.C., Chern, The Development of DDA with Third Order Displacement Function, *Working Forum on the Manifold Method of Material Analysis*, Vol. 1, 342-349, U.S. Army Corps of Engineers, Waterways Experiment Station, Vicksburg, MS, 1997.

Ma, M.Y., M. Zaman, and J.H. Zhu, Discontinuous Deformation Analysis Using the Third Order Displacement Function, *Working Forum on the Manifold Method of Material Analysis*, Vol. 1, 388-394, U.S. Army Corps of Engineers, Waterways Experiment Station, Vicksburg, MS, 1997.

Popov, E.P., *Mechanics of Materials*, Prentice Hall, New York, 1970.

Shi, G.H., Block System Modeling by Discontinuous Deformation Analysis, Topics in Engineering, Volume 11, C.A. Brebbia and J.J. Conner Eds., *Computational Mechanics Publications*, Boston USA, 1993.

Shi, G.H., Modeling Dynamic Rock Failure by Discontinuous Deformation Analysis with Simplex Integration, *Proceedings of the 1st North American Rock Mechanics Symposium*, Austin, TX, 1994.

Shi, G.H., Discontinuous Deformation Analysis – Technical Note, *First International Forum on Discontinuous Deformation Analysis*, June 12-14, 1996, Berkeley, CA, 1996.

Timoshenko, S., *Strength of Material – Part II Advanced Theory and Problems*, Third Edition, D. Van Nostrand Co., Princeton, NJ, 1956.

Timoshenko, S.P., and J.N. Goodier, *Theory of Elasticity*, McGraw-Hall, New York, 1987.